

ELECTRON TRANSPORT AND MOBILITY CALCULATION IN A ALGAAS/GAAS 2DEG BY MONTE CARLO METHOD

Zeki YARAR, Berrin ÖZDEMİR, Metin ÖZDEMİR*

Department of Physics, Çukurova University, 01330 Adana, Turkey

ABSTRACT

We study the transport properties of quasi-two dimensional electrons confined to a modulation doped AlGaAs/GaAs heterostructure. Schrödinger and Poisson equations are solved self consistently to obtain the potential profile formed at the heterojunction. In addition, empty or occupied quantized energy levels, charge carrier concentrations in each occupied level, wave functions corresponding to each level are also calculated. No adjustable parameters are used, it is sufficient to provide only the material parameters and doping profiles across the junction. Once the wave functions are obtained, electron scattering rates based on Born approximation are calculated using a combination of analytical and numerical methods. The scattering rates calculated are those due to remote ionized impurities, acoustic phonons and polar optic phonons. Phonons are assumed to be 3-dimensional and interface roughness scattering and carrier-carrier scatterings are not included. The drift velocities of electrons along the heterojunction plane are obtained as a function of applied electric field at various temperatures and material parameters using ensemble Monte Carlo method. Mobility calculations are carried out as a function of temperature and as a function of the applied field to the electrons. The subband and valley populations of electrons are also obtained. It is found that the two dimensional nature of confined electrons remains only at low temperatures and at low applied fields, at higher fields the electrons are quickly transferred to higher levels and eventually they become three dimensional electrons. High mobility values are obtained at the temperatures and field values where the two dimensional nature of the system is preserved.

Key words: 2DEG, mobility, modulation doping, AlGaAs/GaAs, self consistent

ALGAAS/GAAS YAPISI İÇİN 2BEG’NİN MONTE CARLO YÖNTEMİ İLE ELEKTRON İLETİMİ VE MOBİLİTE HESAPLARI

ÖZET

Modülasyon katkılı AlGaAs/GaAs tipi çoklu yapıların arayüzeyinde oluşan iki boyutlu elektron gazının (2BEG) iletim özellikleri çalışıldı. Çoklu klem arayüzeyinde oluşan potansiyel profilini elde edebilmek için Schrödinger ve Poisson denklemleri sayısal olarak kendi içinde uyumlu olarak çözüldü. Boş veya dolu enerji seviyelerine ek olarak dolu enerji seviyelerinde bulunan elektron yoğunluğu ve her seviyeye karşılık gelen dalga fonksiyonları hesaplanmıştır. Çözümde hiç bir uyum parametresi kullanılmamış, sadece malzeme parametrelerinin verilmesi yeterli olmuştur. Dalga fonksiyonları elde edildikten sonra iki boyutlu elektronların saçılma oranları Born yaklaşımı temel alınarak analitik ve sayısal yöntemlerle hesaplanmıştır. Gözönüne alınan saçılma mekanizmaları eklem ara yüzeyi dışındaki (uzak) iyonize safsızlıklardan saçılma, akustik ve polar optik fonon saçılmalarıdır. Fononların üç boyutlu olduğu kabul edilmiş, taşıyıcı-taşıyıcı ve pürüzlü arayüzey saçılmaları göz önüne alınmamıştır. Monte Carlo yöntemi kullanılarak elektronların çoklu klem düzlemine paralel olarak sürüklenme hızları uygulanan alanın bir fonksiyonu olarak değişik sıcaklık ve malzeme parametre değerlerinde bulunmuştur. Sıcaklığın ve elektronlara uygulanan alanın bir fonksiyonu olarak mobilite hesapları yapılmıştır. Ayrıca elektronların kesikli alt bant ve üç boyutlu vadi dolulukları da elde edilmiştir. Elektronların iki boyutlu doğasının sadece düşük sıcaklıklar ve düşük alanlarda sağlanabildiği, yüksek alanlarda elektronların çabucak daha yüksek seviyelere geçerek üç boyutlu (3D) oldukları bulunmuştur. Sistemin iki boyutlu doğasının korunduğu sıcaklık ve alan değerlerinde yüksek mobilite değerleri elde edilmiştir.

Anahtar Kelimeler: 2BEG, mobilite, modülasyon katkılama, AlGaAs/GaAs, kendi içinde uyumlu

E-posta: metoz@cu.edu.tr

1. INTRODUCTION

Electronic properties of systems confined to lower dimensions have been studied immensely for a long time[1-3]. The transport properties of two-dimensional systems have widely been studied to build high performance electronic devices such as MODFETs (Modulation Doped Field Effect Transistors) which is also called HEMTs (High Electron Mobility Transistors) and optical devices such as lasers and quantum well photo detectors[4]. A typical example is high electron mobility transistors which take advantage of the separation between the electrons and their donor impurities. The conductive channel consists of a single heterojunction, thus the electronic states are quantized, and the electron motion is quasi two-dimensional. This two dimensional electron gas (2DEG) exhibits good transport properties and high electron velocities. A typical method to use in order to understand device physics and to explore possible future device architectures is the Monte Carlo technique[3,5,6]. In this paper we provide an understanding of two dimensional electron transport along the hetero interface formed at a AlGaAs/GaAs junction at various temperatures. The velocity of carriers, the occupancy of quasi two dimensional subband energy levels at the heterojunction and the occupancy of three dimensional valleys in GaAs are provided. Mobility of carriers as function of temperature and applied field are also presented. The paper is organized as follows: In section II a brief account of the self consistent method used in this study and scattering rates that are used in Monte Carlo calculations are presented. Section III presents the results and a discussion. Conclusions are provided in Section IV.

2. THEORY

The geometry of the sample studied is shown in Figure 1. The z -direction is assumed to be the growth direction, namely it is assumed to be perpendicular to the GaAs/AlGaAs layers. The one-dimensional, one electron Schrödinger equation at the AlGaAs/GaAs heterojunction can be written as[7,8]

$$-\frac{\hbar^2}{2} \frac{d}{dz} \left(\frac{1}{m^*(z)} \frac{d}{dz} \right) \Psi(z) + V(z)\Psi(z) = E\Psi(z) \quad (1)$$

where $\Psi(z)$ is the wave function corresponding to quantized levels, E is the energy, V is the one dimensional potential at the hetero interface, \hbar is Planck's constant divided by 2π and $m^*(z)$ is the effective mass of the electrons whose variation along the direction perpendicular to the interface is taken in to account. The one dimensional Poisson equation at the heterojunction can be written as

$$\frac{d}{dz} \left(\epsilon_s(z) \frac{d}{dz} \right) \phi(z) = \frac{-q(N_D(z) - n(z) - N_A(z))}{\epsilon_0} \quad (2)$$

where ϵ_s is the dielectric constant of the material, ϵ_0 is the permittivity of free space, ϕ is the electrostatic potential, N_D is the ionized donor concentration, $n(z)$ is the total two dimensional electron density and N_A is the density of ionized acceptors at the junction. The potential $V(z)$ is related to the electrostatic potential $\phi(z)$ as

$$V(z) = -e\phi(z) + \Delta E_c(z) \quad (3)$$

where ΔE_c represents the conduction band discontinuity at AlGaAs/GaAs hetero interface. The wave function $\Psi(z)$ in equation (1) and the electron density $n(z)$ in equation (2) are related by

$$n(z) = \sum_{k=1}^m \Psi_k^*(z)\Psi_k(z)n_k \quad \text{where } n_k = \frac{m^*}{\pi\hbar^2} \int_{E_k}^{\infty} \frac{1}{1 + e^{(E-E_F)/kT}} dE \quad (4)$$

where E_k is the eigen energy and E_F is the Fermi energy level.

Equations (1) and (2) are discretized using finite difference approximations for derivatives[8,9,10] and an iterative method is used to solve them self consistently. A first guess for $V(z)$ is used to find eigen functions $\Psi_i(z)$ and energy eigen values E_i from (1) and (2). Then electron density $n(z)$ and the electron density n_i in each level are found from equations (4). Next, a new electrostatic potential $\phi(z)$ is determined from the solution of Poisson equation (2) using the computed value of $n(z)$ and the doping profiles. Finally a new potential $V(z)$ is obtained from equation (3). This procedure is repeated until the potential does not vary beyond a predetermined error tolerance. From these solutions one obtains quantized energy levels (empty or occupied), charge carrier concentrations in each occupied level, wave functions corresponding to each level and the potential profile formed at the interface[8,9]. A typical heterostructure and the corresponding potential profile together with the wave functions for the ground and first excited states are shown in Figures 1 and 2, respectively.

The calculation of scattering rates in a quasi-two-dimensional electron gas can be made if the following matrix elements are properly calculated for the subband wave functions. The scattering rate of electrons in the Born approximation is given by[11]

$$W(k) = \frac{2\pi}{\hbar} \frac{\Omega}{(2\pi)^3} \iiint |\langle k' | H' | k \rangle|^2 \delta(E_{k'} - E_k \mp \hbar\omega_0) dq_z q_{\parallel} dq_{\parallel} d\theta \quad (5)$$

where k is the electron wave vector before scattering, k' is the electron wave vector after scattering, q_{\parallel} is the phonon wave vector on the heterojunction plane such that $q_{\parallel}^2 = q_x^2 + q_y^2$ and $q^2 = q_{\parallel}^2 + q_z^2$, q_z is the component of phonon wave vector in the z -direction and H' is the perturbation Hamiltonian corresponding to the scattering mechanism under consideration. The delta function in equation (5) represents energy conservation and the term $\hbar\omega_0$ is the energy of phonons considered. It is now necessary to compute the squared scattering matrix elements appearing in equation (5). For the acoustic phonon scattering due to deformation potential it is given by[11]

$$|\langle k' | H' | k \rangle|^2 = \frac{Z_d^2 k_B T_L}{c_L \Omega} |G_{m,n}(q_z)|^2 \delta(k'_{\parallel} - k_{\parallel} \mp q_{\parallel}) \quad (6)$$

where the proportionality constant Z_d is termed the acoustic deformation potential, T_L is the lattice temperature, k_B is Boltzmann's constant, c_L is the materials elastic constant, ω_0 is the angular frequency of optical phonons assumed to be constant and Ω is the volume of the crystal under consideration, and k_{\parallel} and k'_{\parallel} are respectively, the in plane component of electron wave vector before and after the scattering. Acoustic phonon scattering is assumed to be elastic, i.e. the $\hbar\omega_0$ term in equation (5) is neglected since the energy of acoustic phonons is much less than electron's energy. The term $G_{m,n}(q_z)$ in equation (6) represents the matrix element in the restricted direction (z -direction) and is given by

$$G_{m,n}(q_z) = \int_{-\infty}^{\infty} \Psi_n(z) e^{iq_z z} \Psi_m(z) dz \quad (7)$$

where the range of integration in z -direction does not necessarily extend to $\pm\infty$ since subband wave functions effectively vanish outside a certain region.

Insertion of equation (6) into equation (5) and integration over possible final states, taking into account the energy and momentum conservation, results in the following scattering rates from the m -th subband to the n -th subband

$$W_{m \rightarrow n}(k) = \frac{Z_d^2 k_B T_L m^*}{\hbar^3 c_L} \Phi(m,n) \quad (8)$$

for the acoustic phonons where $\Phi(m,n)$ is given by

$$\Phi(m, n) = \int_{-q_z \max}^{q_z \max} |G_{m,n}(q_z)|^2 dq_z \quad (9)$$

Longitudinal optic phonon scattering of two dimensional carriers is given by[12]

$$W = \frac{\gamma}{2} \int_{-\infty}^{\infty} \frac{\pi |G_{mn}(q_z)|^2}{\sqrt{q_z^4 + 2q_z^2(2k_i^2 - 2m^* \Delta / \hbar^2) + (2m^* \Delta / \hbar^2)^2}} dq_z \quad (10)$$

where $\Delta = E_m - E_n \pm \hbar\omega$ where E_i is the energy of i -th subband and the constant pre factor γ is defined as $\gamma = 2m^* e^2 \omega P / (2\pi)^2 \hbar^2$ with P given by $P = (1/\epsilon_\infty - 1/\epsilon_s)(N_0 + 1/2 \mp 1/2)$. The factor $(N_0 + 1/2 \mp 1/2)$ represents the phonon density within the crystal. The upper sign represents absorption, which reduces the phonon population from (N_0+1) to N_0 , while the lower sign represents emission of a phonon, which increases the number of phonons from N_0 to (N_0+1) .

Finally for remote impurity scattering rate from $k_{||}$ to $k'_{||} = k_{||} + q_{||}$ can be written as[13]

$$W(k_{||}) = \frac{n_{imp}^{(2D)} m^* e^2}{\pi \hbar^3} \int_0^{2k} |\phi_{nm}^{tot}(q_{||})|^2 \frac{dq_{||}}{k_{||} \sqrt{1 - (q_{||} / 2k_{||})^2}} \quad (11)$$

where $\phi_{nm}^{tot}(q_{||})$ is the total induced potential due to remote impurities including screening effects, $n_{imp}^{(2D)}$ is the density of remote impurities per unit area and the range of integration extends up to Fermi wave vector $(k_F)_{||}$ [7,13].

The integrations in equations (7, 9, 10 and 11) are carried out numerically[10]. Using these calculated scattering rates, the drift velocity of electrons along the interface (parallel to the interface) under an applied electric field is investigated by using ensemble Monte Carlo technique[11]. For electrons whose energy increase under the applied field and as a result transfer to three dimensional high energy valleys, three dimensional scattering rates are used. Only the Γ and L valleys of GaAs are considered. The scattering rates considered for the three dimensional electrons are as follows: acoustic, polar and non-polar optical phonon scatterings [14-17]. The selection of scattering processes are carried out as usual [11,17] for a typical Monte Carlo calculation.

3. RESULTS AND DISCUSSION

Our model of modulation-doped GaAs/Al_{0.3}Ga_{0.7}As structure, its self-consistently calculated potential profile and the wave functions for the ground and first excited states are shown in Figures 1 and 2, respectively. A potential difference of 0.5 V is assumed to be applied to 150 Å thick GaAs cap to compensate for the depletion charge layer. The cap is followed by a 200 Å thick doped AlGaAs layer on which a 100 Å un-doped AlGaAs layer is located which is called the spacer. The GaAs base is made as large as possible to obtain convergent results in numerical calculations. The material parameters used in the calculations are as given in Table 1.

Figure 2 shows the calculated subband wave functions at 4.2 K for the lattice matched GaAs/Al_{0.3}Ga_{0.7}As heterostructure with AlGaAs layer donor doping of $1 \times 10^{18} \text{ cm}^{-3}$. The energy levels at this temperature are found to be 33 and 41 meV with respect to potential well minima, respectively for the ground and first excited states. In order to see the effects of various scattering mechanisms on the 'two dimensional electron gas' transport properties, ensemble Monte Carlo simulations are carried out for various electric field values in the range 0.1 to 6 kV/cm applied to the carriers parallel to the hetero interface. Intra and inter subband scattering of electrons between the two dimensional ground and first excited states are considered. Electrons whose energy exceeds the maxima of the conduction band energy on the GaAs side in Figure 2 are assumed to be three dimensional and treated as such. This assumption can be justified due to the closer spacing of the energy levels at high energies, which forms a quasi continuum as in the case of bulk material. Only the two valleys of the conduction band, namely Γ and L valleys of bulk GaAs are considered, the effect of X valley is neglected. Non-parabolicity effects of the bands are considered except for the scattering by polar optical phonons for which the parabolic band model is used.

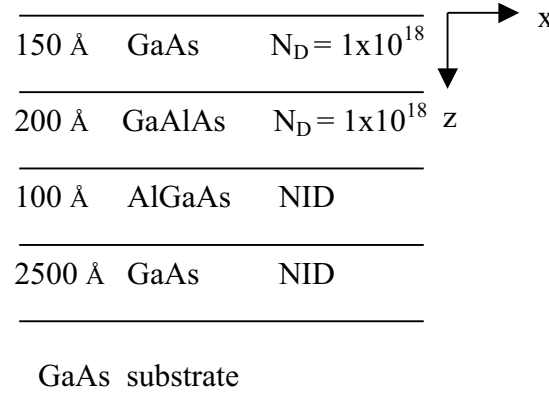


Figure 1. Structure of the quasi two dimensional channel in the modulation doped GaAs/Al_{0.3}Ga_{0.7}As hetero structure. The dielectric constants of AlGaAs and GaAs are 13.1 and 12.9, respectively.

Table 1. The material parameters used in the calculations. The geometry of the sample is shown in Figure 1. m_0 is the mass of free electron (9.1×10^{-31} kg).

Dielectric constant of GaAs	12.9
Dielectric constant of AlGaAs	13.1
Deformation potential for acoustic phonons Z_d (GaAs) (eV)	7.0
Deformation potential for non polar optical phonons D_{eq} (GaAs) (eV/m)	1×10^{11}
Inter valley deformation potential for polar optical phonons D_{ij} (GaAs) (eV)	1×10^{11}
Optical phonon energy, $\hbar\omega_0$ (eV)	0.0354
Effective mass, m^*	$m^*_T = 0.067 m_0$ $m^*_L = 0.35 m_0$
Doping concentration, (cm^{-3})	$N_D = 1 \times 10^{18}$, $N_A = 0$

The trajectory of the electron subjected to two-dimensional scattering mechanisms is followed as a function of time and the electron is placed in the 3D system after the electron's energy exceeds the edge of the conduction band. The scattering mechanisms included in the simulation for the two dimensional (2D) system are acoustic phonon scattering[11], polar optical phonon scattering[12], and remote impurity scattering[7,13]. The scattering mechanisms considered for the three dimensional electrons are acoustic, polar and non-polar optical phonon scatterings [14-17]. Self-consistently calculated electronic states were used in the calculation of the 2D scattering rates.

Velocity-time characteristics for GaAs/Al_{0.3}Ga_{0.7}As modulation doped heterostructures for different applied electric fields are shown in Figure 3. It can easily be seen from the figure that velocities exhibit large transient overshoots at high fields before the steady state values are reached. This is due to the disparity of the momentum and energy relaxation times as functions of electron energy. Transient overshoot is typically observed when the electric field applied is so high that electrons can reach the high-energy region, where the momentum relaxation time is smaller than the energy relaxation time. Later energy relaxation becomes effective so that the distribution function spreads and the drift velocity decreases.

We also note that the velocity overshoot in GaAs/Al_{0.3}Ga_{0.7}As is observed when the electric field is higher than about 0.5 kV/cm as seen in Figure 3. At lower fields it takes a long time to reach the steady state velocity where the velocity makes a couple of oscillations before reaching the steady state value. Further notice that there is a transition region through which the characteristic behavior of the velocity-time changes especially for applied field values above 3 kV/cm. This is apparent for example for an applied field of 4 kV/cm in Figure 3 where there are two peaks

in velocity. The first peak in velocity is due to the two dimensional electrons and the second peak is due to electrons mainly in the Γ valley. The second peak begins to decrease from the moment the L valley begins to be populated.

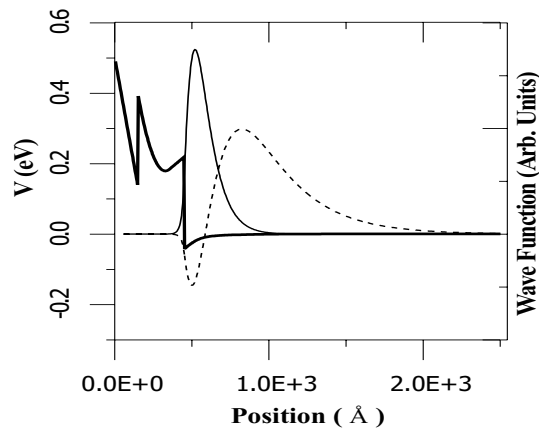


Figure 2. Potential profile (thick line) and wave functions corresponding to ground (thin line) and first excited (dashed line) states.

Let us now consider Figure 3 in some more detail. For all applied field values in that figure, there are two regions for the rate of velocity increase as a function of time until the maximum velocity value is attained. For example, consider the velocity curve that corresponds to an applied field of 0.5 kV/cm. The velocity increases at a specific

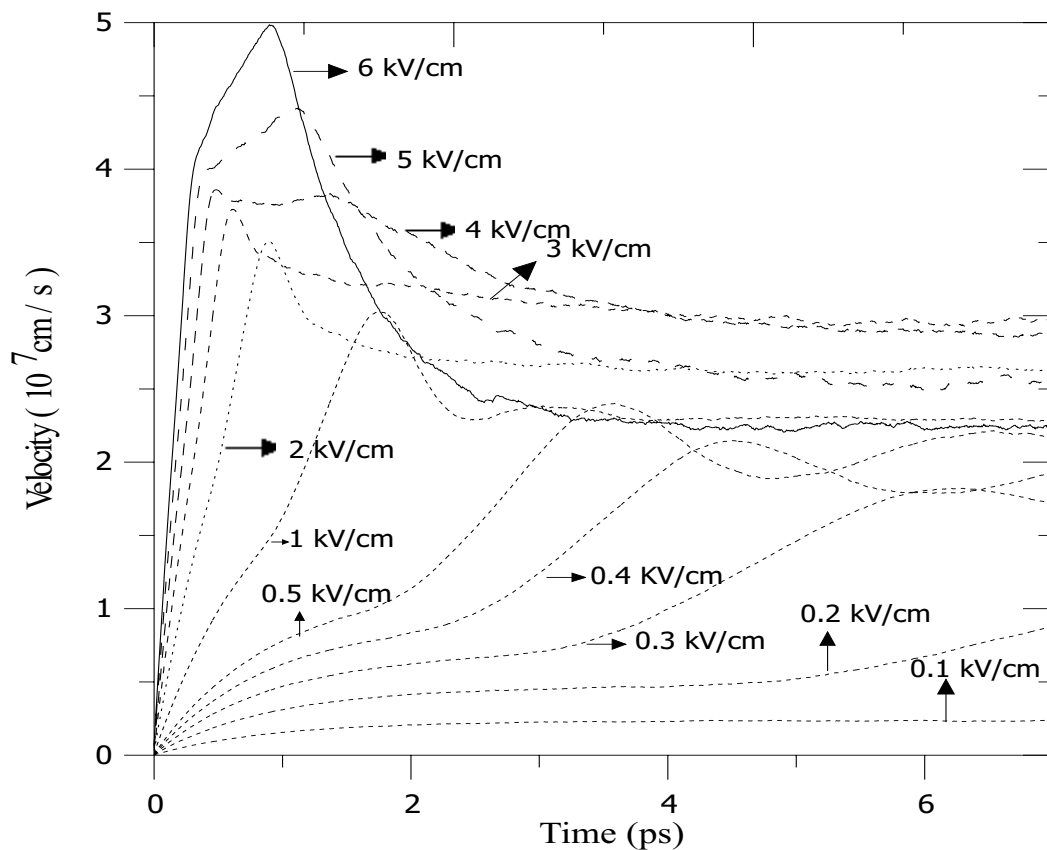


Figure 3. Average velocity of electrons as a function of time at various applied fields parallel to the hetero interface. Note that overshoot effects become apparent at fields above about 0.5 kV/cm. At lower fields, it takes a long time compared to higher fields to reach the steady state velocity. The rate of velocity increase has two regimes, the first one is due to electrons in the ground and first subbands, and the second part is mainly due to electrons in the Γ and L valleys.

rate up to about 2 ps, and then it increases at a different rate after that time until it reaches its maximum value. The former rate is mainly due to electrons in the two dimensional system and the latter is mainly due to electrons that are transferred from two dimensions to the three dimensional Γ valley. This mentioned behavior exists in all curves depicted in Figure 3. Consider the velocity curve for an applied field of 2 kV/cm in Figure 3. The same curve is shown in Figure 4 together with the electron occupancies of two dimensional energy levels and 3D Γ and L valleys of GaAs. As can be seen in Figure 4, the velocity increases until all electrons are transferred from the ground and first subbands to the 3D Γ valley at a certain rate (up to 0.5 ps), and at a different rate after all electrons are transferred to the Γ valley. When the velocity has reached its maximum value in Figures 3 or 4 for an applied field $F=2$ kV/cm, all electrons were already in Γ valley and hence the velocity overshoot observed for the present value of applied field is solely due to electrons in the Γ valley. The L valley is almost empty at this field value. But as the applied field value increases, the two dimensional electrons reach high velocity values in a short time and are transferred from two dimensional system to 3D very quickly. When they become 3D in Γ valley, depending on the field value, either the velocity decreases and reaches the steady state value as for example in the case of an applied

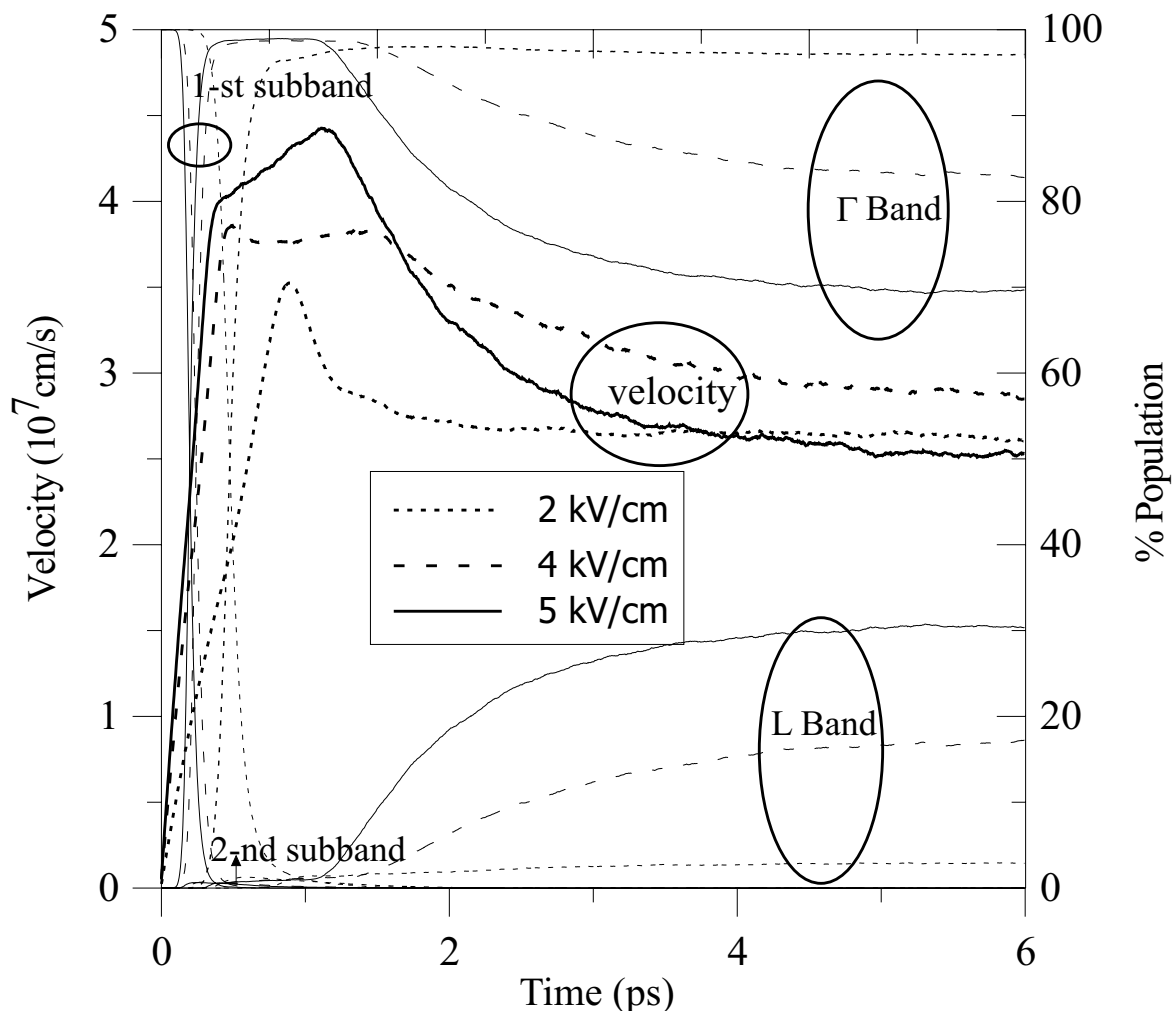


Figure 4. Sub band and Γ and L valley occupancies as a function of time at 4.2 K at applied field values of 2 (short dashed lines) 4 (dashed dotted lines) and 5 kV/cm (solid lines). The average velocity of electrons is also depicted to show the correspondence between level and valley occupancies and electron velocity. Notice the development of a second peak in velocity as the applied field increases.

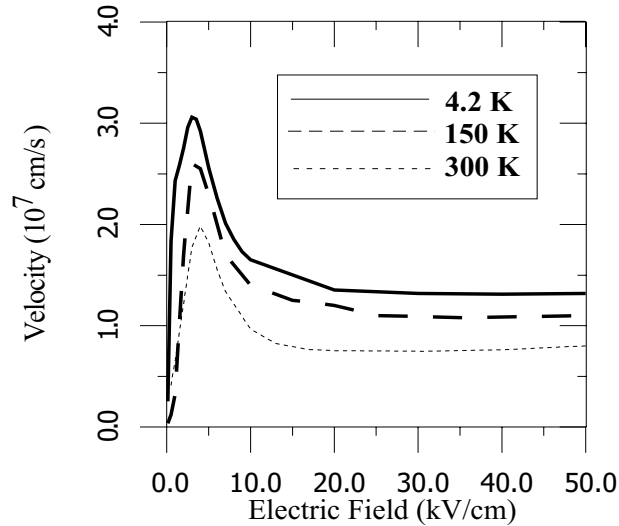


Figure 5. Average electron velocity-electric field curves at different temperatures. The average velocity decreases as the applied field increases, a phenomenon known as negative differential resistance.

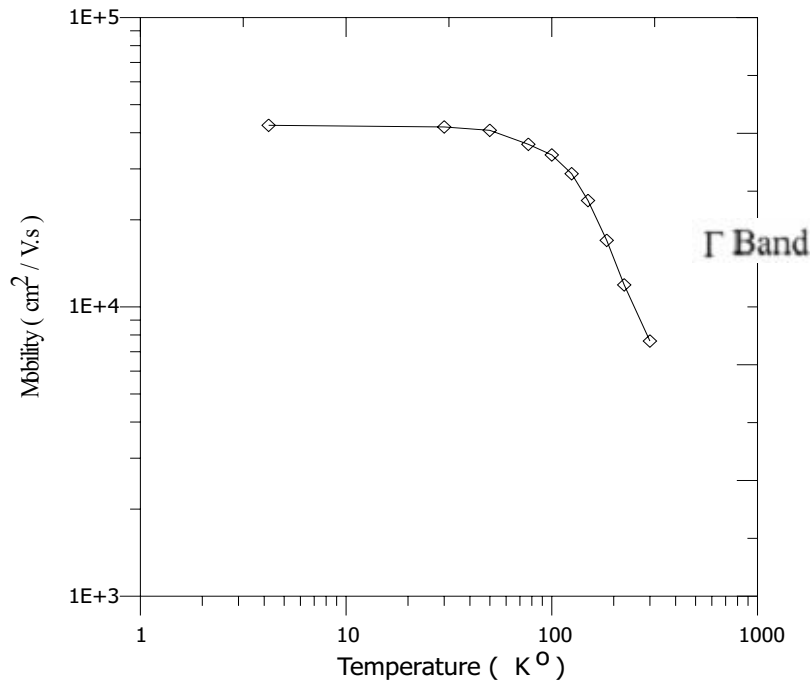


Figure 6. Mobility of electrons as a function of temperature at an applied electric field of 0.5 kV/cm in the absence of remote impurity scattering. High mobility values are attainable only at low temperatures and low applied field values. This is precisely when the system has strictly a two dimensional character.

field of 3 kV/cm in Figure 3, or it continues to increase but at a lower rate and then decrease again as in the case of an applied field of 5 kV/cm in Figure 3. There is a transition region of applied field for these two different behaviors. Consider the velocity curve in Figure 3 for $F=4$ kV/cm where two peaks appear in velocity time characteristic (or dashed dotted line in Figure 4). The two dimensional electrons linearly accelerate with time and reach a maximum velocity. After the Γ valley begins populating, the velocity decreases for a while and begins to increase again and forms the second peak in velocity up until the L valley begin to populate. After this point the

velocity starts to decrease again and after a while reaches a steady state value. At higher fields, for example at an applied field of 5 kV/cm shown in Figure 3 (or solid line in Figure 4) electrons accelerate linearly with time until the two dimensional levels are completely emptied. After the electrons fully become three dimensional by transferring to the Γ valley, their velocity continues to increase linearly but at a lower rate compared to the two dimensional case. Although the electrons spend less time in the Γ valley compared to the case of 4 kV/cm applied field, there is still no decrease in velocity when the electrons are in the Γ valley in this case since the applied field is high enough

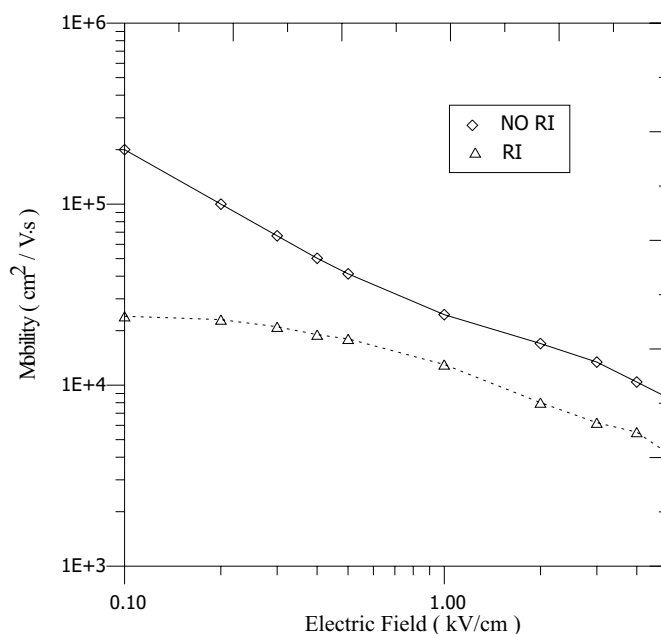


Figure 7. The mobility of electrons as a function of applied field at 4.2 K in the absence (diamonds) and in the presence (triangles) of remote impurity scattering. Remote impurity scattering can reduce the mobility as seen here by a factor of ten. The mobility decreases as the applied field and/or the temperature increases.

to cause the electrons continue to speed up on the average. The decrease in velocity at high F values always occurs after the L valley begins to populate as can be seen in Figure 4. The velocity begin to decrease immediately after the L valley starts getting populated for all cases considered because the effective mass of the electron increases in the L valley. The variation of electron velocity as a function of applied electric field is shown in Figure 5 at various temperatures. For each temperature the velocity increases almost linearly at low fields, reaches a maximum value and then starts to decrease, a property known as negative differential resistance. The maximum speed attained at a given field value decreases as the temperature increases. This can be attributed to the increase in scattering rates due to optical phonons. A small shift of the field to higher values at which the maximum speed is achieved as temperature increases can also be seen in Figure 5. This shift is due to again the increase in optical phonon scattering rates as temperature increases since higher field values are required to attain the maximum speed. Except for low field values, the velocity-field characteristics shown in Figure 5 are all due to electrons transferred to the Γ and L valleys of GaAs since the two dimensional nature of the system considered is maintained only at very low temperatures and low applied field values. When steady state is reached particles are distributed in Γ and L valleys only and the ground and first subbands are emptied completely as can be seen in Figure 4. The occupancy of ground subband decreases sharply shortly after the field is applied and electrons are transferred to higher levels and valleys. Therefore the system is in fact two dimensional for a short duration at moderate field values and it completely becomes a three dimensional system after a while. Therefore a truly two dimensional system is achievable only at low applied field values (< 0.5 kV/cm) and low temperatures (< 100 K) such that an insignificant amount of electrons are transferred to the Γ and L valleys.

Mobility calculations of the system under consideration is carried out at various temperature and applied field values also. The variation of electron mobility as a function of temperature is shown in Figure 6 where remote impurity scattering is not taken into account. The applied field is 0.5 kV/cm so that the system is mainly two dimensional for temperatures up to about 100 K. Beyond this temperature most of the carriers are transferred to the Γ valley and hence the system becomes three dimensional. The mobility is as high as 4×10^4 cm²/V·s at low temperatures but it approaches the bulk value at room temperature since the system becomes completely three dimensional at these temperature values. The variation of mobility as a function of applied field at 4.2 K is shown in Figure 7 in the absence and in the presence of remote impurity scattering. High mobility values are attainable only at low temperatures and low applied fields. As the temperature or applied field increases the mobility decreases and approaches its room temperature bulk values. To see the effect of remote impurity scattering on mobility, the mobility values in the presence of remote impurity scattering for a spacer thickness of 100 Å (see Figure 1) is also calculated as shown in Figure 7. Mobility values without remote impurity scattering are almost ten times higher at low field values. To reduce the effect of remote impurity scattering, the spacer thickness must be increased, but if the spacer is too thick then it becomes hard to create a potential well at the junction where the electrons would be held in two dimensions. Therefore an optimum value of spacer thickness must be chosen where there are enough number of electrons in the two dimensional system and the donor impurities left by the free electrons are considerably far away from the junction not to interfere with the motion of two dimensional electrons.

4. CONCLUSIONS

We presented a numerical study of the transport properties of a two dimensional electron gas formed at a AlGaAs/GaAs heterojunction under an applied field along the interface plane. The potential profile is obtained by the numerical self consistent solution of Schrödinger and Poisson equations. At most two subbands are populated at temperatures and material parameters of interest in this study. Velocity overshoot effects are clearly observed for fields above 0.5 kV/cm. Further the negative differential resistance phenomena resulting from the inter valley scattering for GaAs type materials is also visible at all temperatures studied. Subband level and valley electron occupancies are obtained as functions of transient time at various applied fields and the results are seen to be compatible with average electron velocity variation. The system considered in this study maintains its two dimensional character only at low temperatures and low applied fields. Mobility calculations are also carried out and it is seen that high mobility values are attainable only at low temperatures and low applied field values. To see the effect of remote impurity scattering, two mobility calculations are carried out for a fixed value of spacer thickness. It is seen that the mobility can be ten times higher when remote impurity scattering is not in effect. Further work along these lines for quantum wells is in progress.

ACKNOWLEDGEMENTS

This work is supported in part by Cukurova University Research Fund no: FBE2002D38.

REFERENCES

1. Ando, T., Fowler, A.B. and Stern, F., Rev. Mod. Phys., **54**, 437, 1982.
2. Weisbuch, C., and Vinter, B., Quantum Semiconductor Structures, Academic Press, New York, 1991
3. Jacoboni, C., and Reggiani, L., Rev. Mod. Phys., **55**, 645, 1983.
4. Stern, F., and Howard, W., Phys. Rev., **163**, 816, 1967.
5. Dingle, R., Stormer, H.L., Gossard, A.C., Wiegmann, W., Appl. Phys. Lett., **33**, 665, 1978.
6. Hess, K., Appl. Phys. Lett., **35**, 484, 1979.
7. Bastard, G., Wave Mechanics Applied to Semiconductor Heterostructures, Les Editions de Physique, France, 1988.
8. Tan, I-H., Snider, G.L., Chang, L.D., and Hu, E.L., J. Appl. Phys., **68**, 4071, 1990.
9. Ozdemir, B., Yazar, Z., and Ozdemir, M., Turk J Phys., **28**, 1, 2004.
10. Press, W.H., Teukolsky, S.A., Vetterling, W.T and Flannery, B.P., Numerical Recipes: The Art of Scientific Computing (2nd ed.), Cambridge University Press, USA, 1997.
11. Tomizawa, K., Numerical Simulation of Submicron Semiconductor Devices, Artech House Inc, Japan, 1993.
12. Harrison, P., Quantum Wells Wires and Dots, John Wiley & Sons Ltd., England, 2000.

14. Davies, J.H., The Physics of Low-Dimensional Semiconductors, Cambridge, United Kingdom, 1998.
15. Lundstrom, M., Fundamentals of Carrier Transport, Cambridge, United Kingdom, 2000.
16. Ridley, B.K., Quantum Process in Semiconductors, Clarendon Press, Oxford, 1982.
17. Reggiani, L., Hot Electron Transport in Semiconductors in *Topics in Applied Physics* 58 Ed. by Reggiani, L., Springer-Verlag, New York, 1985.
18. Jacoboni, C., Lugli, P., The Monte Carlo Method for Semiconductor Device Simulation, Springer-Verlag Wien, New York, 1989; Moglestue, C., Monte Carlo Simulation of Semiconductor Devices, Cambridge, London, 1993.